X-671-71-193
PREPRINT

NASA TM X- 65547

AN ABUNDANCE ANALYSIS OF THE PHOTOMETRIC STANDARD 29 Psc

D. A. KLINGLESMITH

MAY 1971

GSFC

GODDARD SPACE FLIGHT CENTER
GREENBELT, MARYLAND

AN ABUNDANCE ANALYSIS OF THE PHOTOMETRIC STANDARD 29 Psc

by

Daniel A. Klinglesmith III*

National Aeronautics and Space Administration
Goddard Space Flight Center
Greenbelt, Maryland

Received: ____________________

ABSTRACT

A fine analysis of the photometric standard star 29 Psc has been performed using flux constant hydrogen-line-blanketed model atmospheres.

The observable quantities, Balmer and Paschen slopes, Balmer discontinuity and H and HeI lines were used to determine the final model parameters: $T_{eff} = 15150^{o}K$, log g = 4.08 and N(He)/N(H) = 0.027.

Lines from 14 elements besides H and He were identified, five elements (C, Mg, Si, Ti and Fe) had a sufficient number of unblended lines with known gf values to attempt an abundance determination.

*Visiting Astronomer, Kitt Peak National Observatory, which is operated by the Association of Universities for Research in Astronomy, Inc., under contract with the National Science Foundation.

I. INTRODUCTION

The star 29 Psc (HD 224926) was chosen by Oke (1964) as a photoelectric standard because it was within 17^{o} of the celestial equator, relatively bright (m_v = 5.1), earlier than A1 and not known to be variable or abnormal. Bless (1969) pointed out that 29 Psc had a small Balmer discontinuity for its spectral type (B8 III) from which it was concluded that the star was similar to helium-rich stars. However, in order to fit all the observable quantities it will be shown that the star is really helium-weak and it is hotter than B8, approximately B6. This paper describes the atmospheric and abundance analyses of 29 Psc. The models used were hydrogen-line-blanketed models (Klinglesmith 1971).

Section II describes the observations that were used; Section III describes the theoretical calculations used to compare with the observations and Section IV describes the fitting procedure used to determine the final model parameters. Sections V and VI describe the abundance and mass-radius determination. The rotational velocity determination and profile fits are discussed in Section VII.

II. THE OBSERVATIONS

a) Spectra

Four coude-spectra were obtained at the Kitt Peak National Observatory 84-inch telescope on January 25 and 26, 1970. The spectra were taken on IIaO plates and developed with the necessary calibration plates in D-76 for 12 minutes. Table 1 lists the pertinent data for the exposures. The linear dispersion was 8.9 Å/mm with a resolving power of approximately 25,000. The useful spectral range was λ3700 to λ4800. The density was recorded on magnetic tape with a

Joyce-Lobel microdensitometer and converted to intensity in the computer. The four separate spectra were averaged to form one composite spectrum. It was possible to measure equivalent widths as small as 40 milliangstroms. Table 2 lists the observed lines with their identifications and equivalent widths. Lines for which there are no equivalent width measurements were considered weak enough to be seen but not measured.

b) Continuous Energy Distribution

Since 29 Psc is a photoelectric standard, there exists good continuum data in the literature (Oke 1964 and Hayes 1970). The two sets of data are essentially in agreement (Hayes, Oke and Schild 1970).

Figure 1 shows the original data from Hayes (1970) and the renormalization for the current calibration of Vega (Oke and Schild 1970). It can be seen that the revision has the largest effect on the Balmer slope, in fact, changing the sign of the Balmer slope from negative to positive. This permits a consistent temperature to be determined from the 3 continuum observables as will be described in Section IVa.

c) Colors

Crawford (1963) obtained UBV and Hβ colors for 29 Psc: U-B = -0.50, B-V = -0.3, Hβ = 2.708, $E_{(U-B)}$ = 0.0 and A_λ = 0.0. From its position in the color-color and the Hβ vs. $(U-B)_o$ plots (Figure 1 and 2 of Crawford's paper) it can be inferred that 20 Psc is indeed a B6 not a B8 star. Irwin (1961) used 29 Psc as a comparison standard for his Southern Cepheid Photometry and did not find any indication of variation in the colors.

III. THEORETICAL CALCULATIONS

The model stellar atmospheres used in the analysis were flux constant, hydrogen line-blanketed models (Klinglesmith 1971). The usual assumptions of hydrostatic, radiative and thermodynamic equilibrium were made. The sources of opacity included were the bound-bound transitions of the Lyman and Balmer series of hydrogen, the bound-free and the free-free transitions of hydrogen, helium and their ions both positive and negative.

The line profiles and equivalent widths of H_γ, H_δ and H_ϵ were computed using the "ESW" formulation of Stark broadening and the HeI lines were computed using Stark broadening data from 2 different sources: for λ4121 and 4713 from Griem (1964) and for λ4026, 4388 and 4471 from Barnard, Cooper and Shamey (1969).

The line absorption coefficient for the metal lines used in the abundance analysis was a Voight function. The damping constants used are listed in Table 3 along with the other atomic data. In each case it was attempted to use the most realistic value that was available.

The theoretical Balmer discontinuity was defined as

$$D_{3647} = -2.5 \log_{10} \left(F_\nu(3647^+)/F_\nu(3647^-)\right)$$

where $\log F_\nu$ (3647^+) was obtained by linear extrapolation using $\log F_\nu$ (4546) and $\log F_\nu$ (4217). The rather peculiar wavelengths result from the quadrature points used in the model atmosphere calculations; λ4217 is halfway between H_δ and H_γ and λ4586 is halfway between H_γ and $H\beta$.

The Balmer and Paschen slopes are defined as

$$\Phi_B = -2.5 \log_{10}\left(F_\nu(3647^-)F_\nu(3421^+)\right)/\Delta\lambda(\mu);\ \Delta\lambda = 0.0226\ \mu$$

$$\Phi_P = -2.5 \log_{10}\left(F_\nu(5508)/F_\nu(5050)\right)/\ \Delta\lambda(\mu);\ \Delta\lambda = 0.0458\ \mu$$

Again, the peculiar wavelengths are a result of the quadrature points used in the model calculations.

IV. FITTING THE OBSERVABLES

The observable quantities: Balmer and Paschen slopes, Balmer discontinuity, and equivalent widths of the hydrogen and helium lines were measured in a manner identical to the way they were computed from the theoretical model atmospheres. The theoretical quantities were plotted as a function of effective temperature for each log g with one curve for each helium to hydrogen ratio. A plot of the T_{eff} - log g pairs that fit each of the observables represents the locus of the models that would give the observed value; again, one curve for each abundance. The loci have different slopes in the T_{eff} - log g plane due to the different T_{eff} - log g dependence of each observable. However, the loci of a given observable for different helium to hydrogen ratios are essentially parallel. The intersection of two or more loci for a given helium to hydrogen ratio determines a model that fits those two or more observables. Figure 2 shows these loci for 29 Psc. The individual loci will be described in the following sections.

a) The Continuum Observables

The values for the continuum observables for the revised photoelectric energy distribution of 29 Psc (Figure 1) are $D_{3647} = -0.71$; $\phi_B = 1.80$ and $\phi_P = 2.68$.

Each one of the 3 continuum observables gave a similar loci, i.e. no gravity dependence and very little temperature dependence for a given helium to hydrogen ratio, however, there is a temperature spread of about 1000^{o}K when the helium to hydrogen ratio varies from 0 to 1.5. Hence, the loci of each observable at one helium to hydrogen ratio were averaged together. Figure 2 shows the resultant "averaged loci". They are labeled H-continuum.

b) Hydrogen Lines

The equivalent widths of the hydrogen lines on the other hand do show a dependence on both T_{eff} and log g as well as abundance. Three lines were used (H_γ, H_δ and H_ϵ) and their individual loci were averaged for each helium to hydrogen ratio. At a given log g the total spread in temperature between the loci of H_γ, H_δ and H_ϵ was 800°K or less. The average of the 3 loci were plotted in Figure 2 - labeled H-lines.

At this point it is possible to draw a line (marked HLC in Figure 2) that shows the interceptions of the hydrogen line loci with the hydrogen continuum loci. This line indicates the parameters of the models that would best fit the hydrogen observables. Notice that the helium to hydrogen ratio would vary along the line.

c) The Helium Lines

The equivalent widths of 5 HeI lines for which good Stark broadening data exist were also used to obtain "averaged loci" at four helium to hydrogen ratios (0.013, 0.028, 0.125 and 1.5). The equivalent widths for the two smallest ratios were obtained by using a pure hydrogen atmosphere and assuming the helium was an impurity. The five lines were 4026, 4388, 4471, 4121 and 4713. The individual loci at a given helium to hydrogen ratio had a spread of ~ 1500°K at a given log g.

The dashed line marked HHE is the line of intercepts between the hydrogen lines and the helium lines. The intersection of the lines HHE and HLC at T_{eff} = 15150°K and log g = 4.08 determine the effective temperature and log g for 29 Psc. In order to determine the helium to hydrogen ratio at this T_{eff} and log g, three models were computed with the previously determined T_{eff} and log g and different helium to hydrogen ratios (0.013, 0.028 and 0.044). The profiles and equivalent

widths of the 5 HeI lines were recomputed for each model. The variation of W_λ with N(He)/N(H) is shown in Figure 3. The crosses indicate the observed W_λ for each of the lines. The individual N(He)/N(H) and these averages are given in Table 3. Thus, from the hydrogen continuum, the hydrogen lines and the helium lines a final model with the parameters $T_{eff} = 15150 \pm 700$; $\log g = 4.08 \pm 0.15$ and N(He/N(H) = 0.027 ± 0.012 has been determined.

V. ABUNDANCE ANALYSIS

Using the same techniques that have been used in previous analyses (Hunger and Klinglesmith 1969 and Klinglesmith, Hunger, Bless and Millis 1970) the abundances of five elements were determined. The only new feature of analysis is the inclusion of variable partition functions (Sparks and Fischel 1971). Table 4 lists the lines used in the abundance analysis, their atomic data and the derived mass fractions. Table 5 gives the relative number fractions $\mathcal{E}_i$ for 29 Psc and a normalized log N_i for 29 Psc, B stars (Aller 1961) and the cosmic abundances (Allen 1963). From this, we can see that only the carbon abundance appears normal. Magnesium is underabundent (only one line was used) whereas Si, Ti and Fe are overabundant by about an order of magnitude or more. The spread in the individual determination for Ti and Fe lines indicates that the gf values and/or the damping constants are still not well enough known.

VI. MASS AND RADIUS

There is no direct distance measure for 29 Psc, however, two indirect methods can be used in order to derive an estimate of the mass and radius. The spectral type that corresponds to 15000°K is B6 and the luminosity that corresponds to log g = 4 is V or IV (Blaauw 1963). This implies a mean M_v of -1.1 and since there is no absorption (Crawford 1963) a distance of

$\approx$ 175 parsecs results. Using Petrie's (1958a, b) H_γ vs. luminosity relation one obtains $M_v \approx -0.8$ and a distance of 150 parsecs. The bolometric correction for the final model is -1.32 which gives an average $M_{Bol} = -2.32$. The mass and radius can be determined from the relations (see Klemola, 1961)

$$5 \log R = 42.4 - 10 \log T_{eff} - M_{Bol}$$

and

$$\log M = \log g + 2 \log R - 4.38.$$

This results in $M \approx 7.4\ M_\odot$ and $R \approx 3.8\ R_\odot$. These values are consistent with the mass and radius of a normal B star and should not be interpreted any more strongly than that.

VII. ROTATIONAL VELOCITY

In order to attempt profile fits it is necessary to know the rotational velocity or rather $v_r \sin i$. For 29 Psc this was determined from the MgII 4481 line. First, the abundance of Mg was determined from the equivalent width. Then, with that abundance, an unrotated profile was computed and rotated using the expression given by Pecker and Schatzman (1959),

$$P_r(\lambda) = \int_{-1}^{+1} P_u\left(\lambda \left\{1 - \frac{v_r \sin i}{c} x\right\}\right) \frac{\pi/2(1-x^2)^{\frac{1}{2}} + \frac{\beta}{2}(1-x^2)}{1 + \frac{2}{3}\beta}\, dx.$$

This expression describes the effect on the unrotated profile, P_u, on a spherical star with a linear limb-darkening law, where β is the limb-darkening coefficient.

The MgII 4481 line was rotated at 50, 60 and 70 km/sec and the best fit was obtained with 60 km/sec.

Using these same values the HeI and hydrogen lines were also rotated, Figure 4 shows the results. For the HeI lines 3 values of N(He)/N(H) are shown at each $v_r \sin i$. The best

fit is obtained for a N(He)/N(H) $\approx$ 0.028 and V_r sin i = 60 km/sec. For the H lines only the 60 km/sec profiles are shown. The two calculated profiles represent N(He)/N(H) of 0.013 and 0.125. The fit is good in the wings but the observed cores are still too deep.

The metal lines whose equivalent widths were greater than 0.1Å were also rotated and again 60 km/sec was the v_r sin i that was obtained if the unrotated profile had the abundance determined from the equivalent width measurement.

VIII. CONCLUSIONS

The standard LTE type of model atmosphere abundance analysis has shown that the observed data for 29 Psc can be consistently fitted by a model in which helium is underabundant by a factor of 4 compared to the current estimate for N(He)/N(H) = 0.106 (Leckrone 1971) for normal main-sequence stars. Also the overabundance of the Fe group elements along with the underabundance of helium are consistent with the idea that 29 Psc is a hot Ap star.

REFERENCES

Allen, C.W. 1963, Astrophysical Quantities (London: Athlone Press).

Aller, L.H. 1961, The Abundance of the Elements (New York: Interscience Publishers).

Barnard, A.J., Cooper, J., and Shamey, L.H. 1969, Astron. & Astrophys., 1, 23.

Blaauw, A. 1963, Basic Astronomical Data (Univ. of Chicago. Press, Chicago: ed. Aa. Strand).

Bless, R.C. 1968, private communication.

Crawford, D.L. 1964, Ap.J., 137, 530.

Edmonds, F.M., Jr., Schlüter, H., and Wells, D.C., III 1967, Mm. R.A.S., 71, 271.

Griem, H.R. 1964, Plasma Spectroscopy, (New York: McGraw Hill).

Hayes, D.S. 1970, Ap.J., 159, 165.

Hayes, D.S., Oke, J.B., and Schild, R.E. 1970, Ap.J., 162, 361.

Hunger, K. and Klinglesmith, D.A. 1969, Ap.J., 157, 721.

Irwin, J.B. 1961, Ap.J. Suppl., 6, 253.

Klemola, A.R. 1961, Ap.J., 134, 130.

Klinglesmith, D.A. 1966, Ph.D. Thesis, Indiana University.

Klinglesmith, D.A., Hunger, K., Bless, R.C., and Millis, R.L. 1970, Ap.J., 159, 513.

Klinglesmith, D.A. 1971, Hydrogen Line-Blanketed Model Atmospheres, NASA SP-3065, (U.S. Govt. Printing Office, Wash. D.C.).

Leckrone, D.S. 1971, Astron. & Astrophys., in press.

Oke, J.B. 1964, Ap.J., 140, 689.

Oke, J.B. and Schild, R.E. 1970, Ap.J., 161, 1015.

Pecker, J.C. and Schatzman, E. 1959, Astrophysique Generale, Masson, Paris.

Petrie, R.M. 1958a, M.N., 118, 80.

__________ 1958b, Contr. Dom. Ap. Obs., No. 61.

Sparks, W.M. and Fischel, D. 1971, Ap.J., 164, 359.

FIGURE CAPTIONS

Fig. 1 - The emergent flux for 29 Psc. The dots are Hayes original data, the crosses are Hayes data corrected for the new calibration of Vega by Oke and Schild.

Fig. 2 - Atmospheric parameter determination; see text for description. The final model has T_{eff} = 15150 and log g = 4.08.

Fig. 3 - The equivalent widths of the HeI lines as a function of the Helium to Hydrogen ratio. The crosses are the observed values of W_λ for 29 Psc.

Fig. 4 - Helium and Hydrogen line profile fits for 29 Psc. For the 5 HeI lines, 3 values of N(He)/N(H) are plotted 0.013(———), 0.028(---) and 0.043(···). The computed profiles have been rotated to the value shown over the curves. The broad line is the observed curve. The hydrogen lines are rotated to 60 km/sec and shown for 2 N(He)/N(H) (0.013 and 0.125). indicates the observations.

TABLE 1

Photographic Data for 29 Psc

Plate	Date	Time (U.T.)	Length (Min)
D2061a	Jan. 25, 1970	$01^h\ 46^m$	17
D2062a	Jan. 25, 1970	$02^h\ 15^m$	16
D2062b	Jan 25, 1970	$02^h\ 44^m$	24*
D2074a	Jan. 26, 1970	$01^h\ 47^m$	36*

*longer exposures due to variable clouds

TABLE 2

Lines Found in 29 Psc

λ_{OBS}	λ_{RMT}	Element	#	W_λ
3691.52	3691.557	H	18	0.171
3696.88	3697.154	H	17	0.346
3703.76	3703.855	H	16	0.617
3711.92	3711.973	H	15	0.980
3721.72	3721.940	H	14	1.736
3734.14	3734.370	H	13	2.512
3736.80	3736.901	Ca II	(3)	
3750.08	3750.154	H	12	3.477
3759.36	3759.29	Ti II	(13)	0.084
3761.28	3761.320	Ti II	(13)	0.039
3770.72		H	II	4.738
3797.94		H	10	5.958
3819.70	3819.606	He I	(22)	0.260
	3819.761	He I	(22)	
3835.36	3835.386	H	09	7.116
	3843.64	Cr I	(87)	
3845.04	3845.21	S II	(23)	
3848.98	3848.96	Cr I	(69)	0.018
3853.84	3853.657	Si II	(1)	0.072
3856.08	3856.021	Si II	(1)	0.173
3862.72	3862.592	Si II	(1)	0.145
3867.68	3867.477	He I	(20)	0.070
	3867.631	He I	(20)	
3870.08	3807.06	Al II	(74)	0.035
3889.12	3889.051	H	08	7.754
3894.0	3894.035	Cr II	(23)	
3900.56	3900.546	Ti II	(34)	0.038
	3900.680	Al II	(1)	
3905.60	3905.52	Si I	(3)	
3906.72	3906.95	S II	(3)	
3908.88	3908.76	Cr I	(23)	
3913.44	3913.46	Ti II	(34)	0.065
3919.12	3918.977	C II	(4)	0.037
3920.64	3920.677	C II	(4)	0.148
3924.96				
3933.670	3933.664	Ca II	(1)	0.152
3968.50	3968.47	Ca II	(1)	
3970.02	3970.074	H	07	8.016
3978.90	3978.87	C II	(37)	
4002.84	4002.940	V II	(9)	
4009.6	4009.27	He I	(55)	0.249

λ_{OBS}	λ_{RMT}	Element	#	W_λ
4026.40	4026.189	He I	(55)	0.673
	4026.362	He I	(55)	
4076.4	4076.0	C II	(36)	0.034
4101.76	4101.737	H	06	7.937
4121.90	4120.821	He I	(16)	0.089
	4120.993	He I	(16)	
4122.72	4122.638	Fe II	(28)	
4128.08	4128.053	Si II	(3)	0.135
4130.95	4130.884	Si II	(3)	0.132
4143.93	4143.759	He I	(53)	0.271
4169.00	4168.971	He I	(52)	0.039
4173.44	4173.537	Fe II	(27)	0.073
	4173.510	N II	(50)	
4178.32	4178.39	V II	(25)	
4179.05	4178.855	Fe II	(28)	0.095
4206.00	4205.92	Ti II	(3)	
4233.29	4233.167	Fe II	(27)	0.064
4267.15	4267.02	C II	(6)	0.067
	4267.27	C II	(6)	
4303.2	4303.166	Fe II	(27)	0.066
4340.48	4340.468	H	05	8.310
4351.53	4351.764	Fe II	(27)	0.032
4385.4	4385.38	Fe II	(27)	0.125
4387.6	4387.928	He I	(51)	0.234
4395.28	4395.031	Ti II	(19)	0.061
4416.84	4416.817	Fe II	(27)	0.063
4437.66	4437.549	He I	(50)	0.046
4469.96	4469.92	He I	(15)	
4471.52	4471.477	He I	(14)	0.346
	4471.688	He I	(14)	
4475.12				
4481.26	4481.128	Mg II	(4)	0.263
	4481.327	Mg II	(4)	
4488.2	4489.185	Fe II	(37)	
4508.18	4508.283	Fe II	(38)	0.045
4515.36	4515.237	Fe II	(37)	
4522.6	4522.634	Fe II	(38)	0.041
4549.46	4549.467	Fe II	(38)	0.108
4555.92	4555.890	Fe II	(37)	0.035
4583.76	4583.829	Fe II	(38)	0.087
4629.36	4629.336	Fe II	(37)	0.082
4713.5	4713.143	He I	(12)	0.041
	4713.71	He I	(12	

TABLE 3

N(He)/N(H) from W_λ(HeI)

λ	N(He)/N(H)
4026	0.036
4121	0.037
4388	0.028
4471	0.015
4713	0.010

$\langle N(He)/N(H) \rangle = 0.027 \pm 0.012$

TABLE 4 - Lines Used for Abundance Analysis

Atom & Ion	Multiplet Number	λ_{RMT}	Transition	E.P. (ev)	gf	$\gamma x10^{-8}$	W_{λ}(Å)	Z x 10^3	$<Zx10^3>$
								(by mass)	
C II	4	3918.97	$3p^2P^0 - 4s^2S$	16.327	0.286	2.62	0.037	2.5	
	6	4267.27	$3d^2D - 4f^2F^0$	18.041	5.34	2.44	0.067	1.9	2.2
Mg II	4	4481.327 .128	$3^2D - 4^2F^0$	8.83	9.55	8.8	0.263	0.046	0.046
Si II	1	3862.60	$3^2D - 4^2P^0$	6.856	0.228	0.250	0.145	2.5	
		3856.02		6.854	0.124	0.280	0.173	9.9	
		3853.66		6.854	0.0056	0.0280	0.072	5.2	
	3	4130.89	$3^2D - 4^2F^0$	9.834	2.899	1.42	0.132	1.9	
		4128.07		9.832	2.040	1.32	0.135	2.9	4.5
Ti II	13	3759.29	$a\,^2F - z^2F$	0.607	2.20	1.25	0.084	0.27	
		3761.32		0.574	1.70	1.36	0.039	0.03	
	19	4395.28	$a\,^2D - z^2F^0$	1.084	0.35	0.24	0.061	0.27	
	34	3900.546	$a\,^2G - z^2G^0$	1.130	0.96	0.42	0.038	0.03	
		3913.46		1.115	0.87	0.475	0.065	0.21	0.16
Fe II	27	4416.817	$b\,^4P - z^4D^0$	2.77	0.0081	1.14	0.063	2.4	
		4351.764		2.69	0.0254	1.17	0.032	1.6	
		4303.166		2.69	0.0100	1.20	0.066	2.6	
		4233.167		2.57	0.0037	1.24	0.064	0.8	
		4173.450		2.57	0098	1.27	0.073	7.4	
	28	4178.855	$b\,^4P - z^4F^0$	2.57	0.0100	1.27	0.095	8.4	
	37	4629.336	$b\,^4F - z^4F^0$	2.79	0.0288	1.06	0.082	2.5	
		4555.890		2.82	0.0234	1.07	0.035	0.3	
	38	4583.829	$b\,^4F - z^4D^0$	2.79	0.0562	1.06	0.087	4.4	
		4549.467		2.83	0.0467	1.06	0.108	10.0	
		4522.634		2.83	0.0309	1.08	0.41	3.5	
		4508.283		2.84	0.0166	1.08	0.045	8.4	4.3

TABLE 5

Number Fractions ε_i and log N_i

Element	$\varepsilon_i (\Sigma\varepsilon_i = 1.0)$	29 Psc	B stars	Cosmic
			log N_i	
H	0.975	12.00	12.00	12.00
He	2.45×10^{-2}	10.40	11.21	11.16
C	2.04×10^{-3}	8.32	8.30	8.48
Mg	2.08×10^{-6}	6.33	7.95	7.46
Si	1.77×10^{-4}	8.26	7.45	7.47
Ti	3.70×10^{-6}	6.58		4.82
Fe	8.50×10^{-5}	7.94		6.90

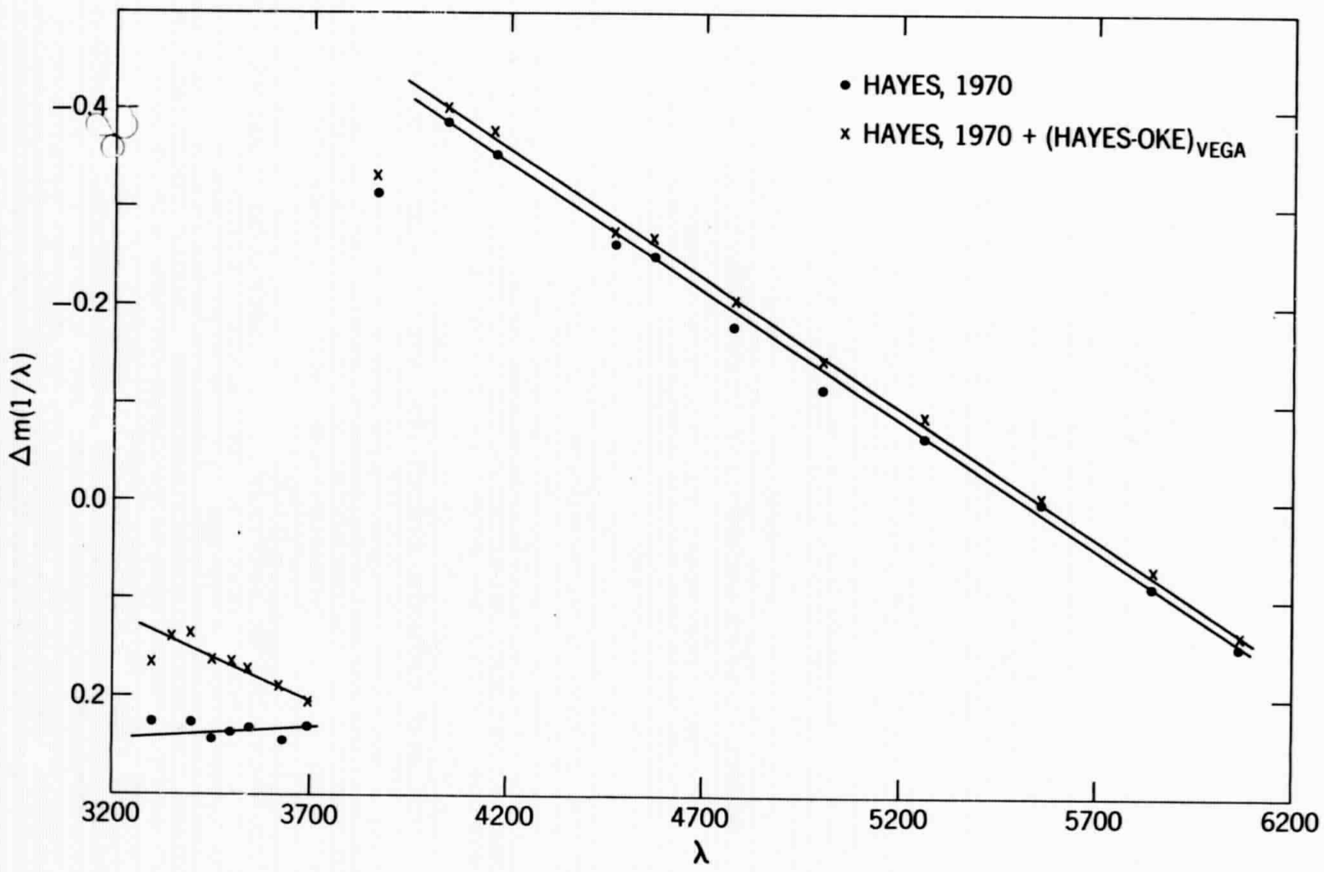

• HAYES, 1970
× HAYES, 1970 + (HAYES-OKE)VEGA
−0.4
−0.2
0.0
0.2
Δm(1/λ)
3200
3700
4200
4700
5200
5700
6200
λ

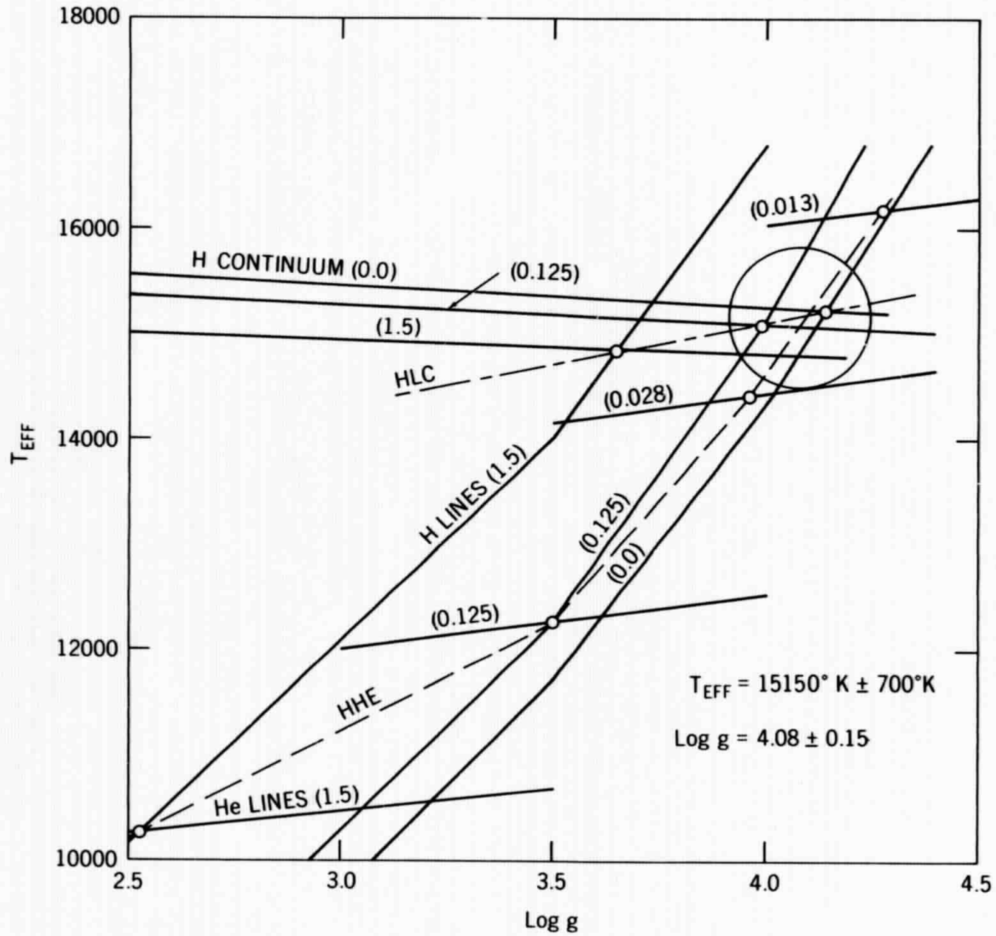

18000
16000
14000
12000
10000
T_EFF
2.5
3.0
3.5
4.0
4.5
Log g
H CONTINUUM (0.0)
(0.125)
(1.5)
HLC
(0.013)
(0.028)
H LINES (1.5)
(0.125)
(0.0)
(0.125)
HHE
He LINES (1.5)
T_EFF = 15150° K ± 700°K
Log g = 4.08 ± 0.15

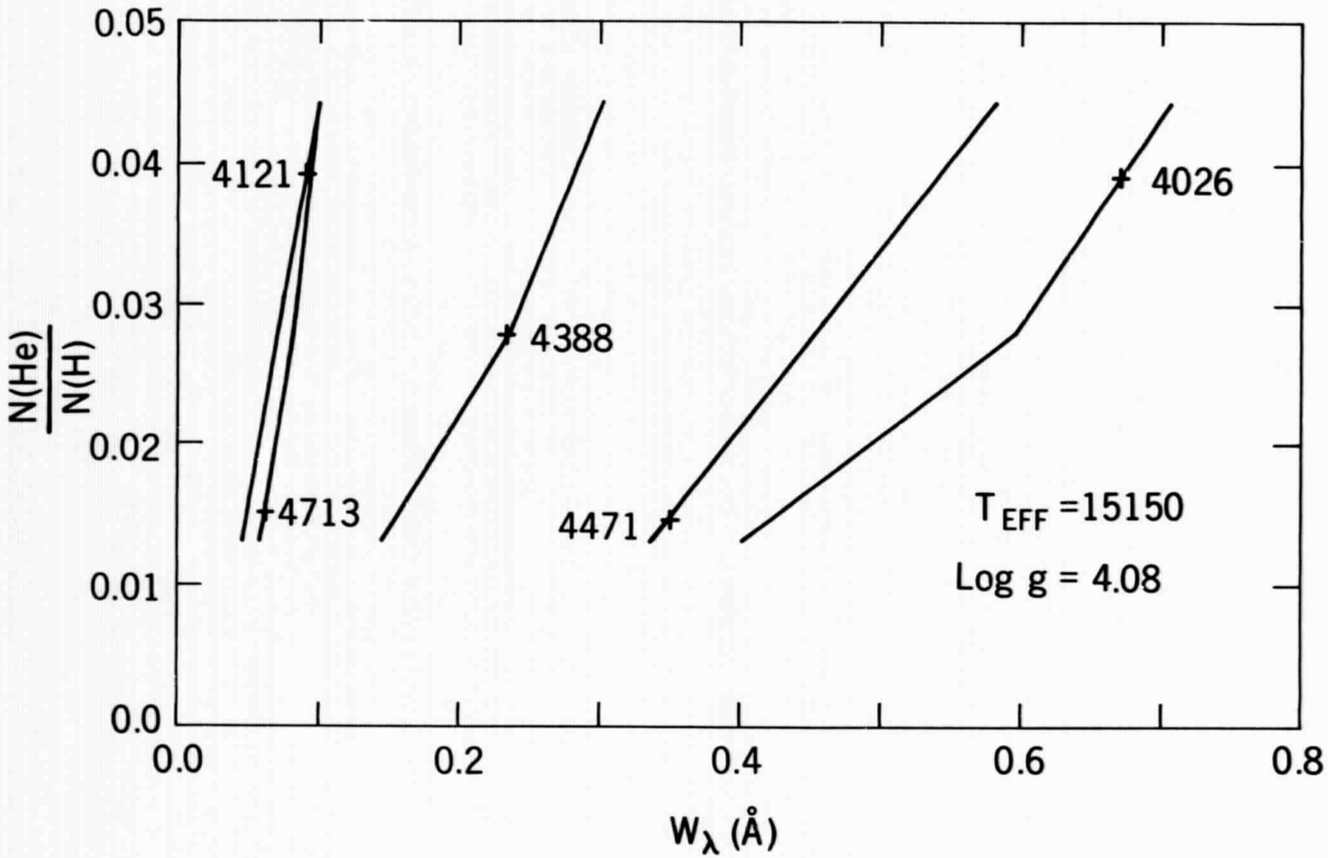

0.05
0.04
0.03
0.02
0.01
0.0
N(He)/N(H)
0.0
0.2
0.4
0.6
0.8
W_λ (Å)
4121
4713
4388
4471
4026
T_{EFF} =15150
Log g = 4.08

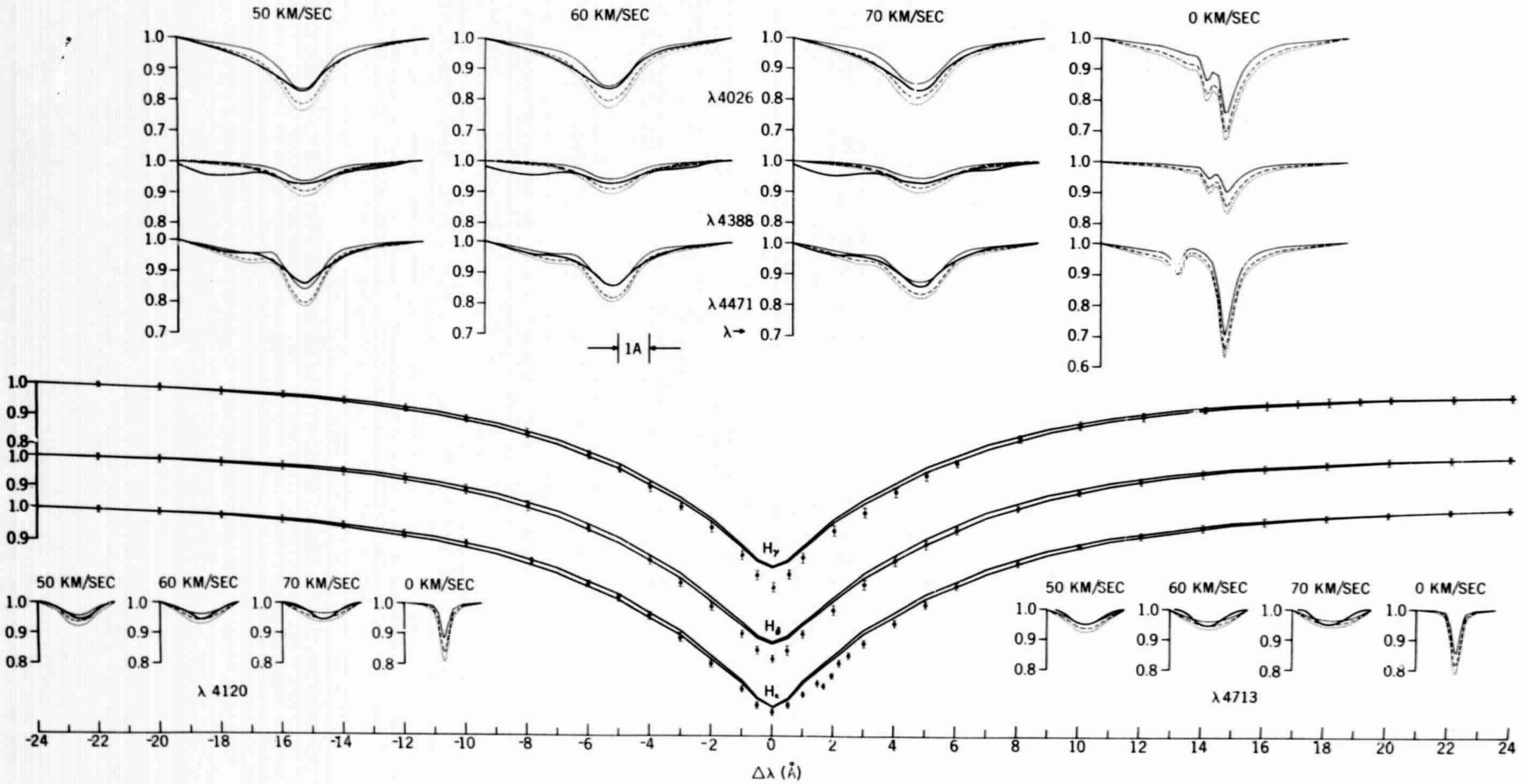

50 KM/SEC
60 KM/SEC
70 KM/SEC
0 KM/SEC
λ4026
λ4388
λ4471
λ→
1A
H_γ
H_δ
H_ϵ
λ 4120
λ4713
Δλ (Å)